und den Spezialfall der Punktlage 48(*f*) in *Ia3d* (ein Freiheitsgrad). Schwieriger wird im dreidimensionalen Fall vor allem die anschauliche Darstellung der Ergebnisse, da einerseits die zu betrachtenden Parameterräume höhere Dimensionszahlen aufweisen können (maximal 8 für $P\bar{1}$), andererseits die topologische Symbolisierung nicht auf so einfache Weise wie im Falle der Kreispackungen möglich ist.

Mein Dank gilt an dieser Stelle Herrn Prof. Dr E. Hellner, der die Anregung zur Beschäftigung mit diesen Problemen gegeben hat und darüber hinaus durch zahlreiche Diskussionen zum Fortschritt der Arbeit beigetragen hat.

Literatur

BURZLAFF, H., FISCHER, W. & HELLNER, E. (1968). *Acta Cryst.* A**24**, 57.
HEESCH, H. & LAVES, F. (1933). *Z. Kristallogr.* **85**, 443.
HERMANN, C. (1960). *Z. Kristallogr.* **113**, 142.
Internationale Tabellen zur Bestimmung von Kristallstrukturen (1935). 1. Aufl. Band 1.
LAVES, F. (1931*a*). *Z. Kristallogr.* **76**, 277.
LAVES, F. (1931*b*). *Z. Kristallogr.* **78**, 208.
NIGGLI, P. (1927). *Z. Kristallogr.* **65**, 391.
NIGGLI, P. (1928). *Z. Kristallogr.* **68**, 404.
NOWACKI, W. (1935). *Homogene Raumteilung und Kristallstruktur.* (Diss.) Zürich.
SINOGOWITZ, U. (1939). *Z. Kristallogr.* **100**, 461. (Diss.)
SINOGOWITZ, U. (1943). *Z. Kristallogr.* **105**, 23.

Acta Cryst. (1968). A**24**, 81

Many-Beam Dynamical Theory of the Line in the Middle of a Kikuchi Band

BY YOSHIRO KAINUMA AND MOTOKAZU KOGISO

Department of General Education, Nagoya University, Nagoya, Japan

(*Received* 10 *June* 1967)

The unindexed line which runs along the middle line of a Kikuchi band is explained in the case of the 200 band from magnesium oxide by the theory of Kikuchi patterns [Kainuma, *Acta Cryst.* (1955) **8**, 247]. The intensity profile across the line is estimated without solving the equation of the dispersion surface, by using a matrix formulation of the many-beam dynamical theory. In the estimation, the 000, 200 and 400 reflexions of elastically scattered waves and the $\bar{2}00$, 000 and 200 reflexions of inelastically scattered waves are taken into account. The result of the calculation agrees qualitatively with the observation.

Introduction

Many researchers on electron diffraction have observed a line which runs along the middle line of a Kikuchi band. For example, Ichinokawa & Fukano (1952) observed it for molybdenite, Pfister (1953) for lead iodide, and Uyeda & Nonoyama (1965*b*) for magnesium oxide. The line cannot be indexed as a Kikuchi line. It appears as an excess, deficient or excess–deficient line according to experimental conditions. The excess line is black, and the deficient line white, on photographic plates. The excess–deficient line is black on one side and white on the other side of the line. In this article, the unindexed line is explained by the theory of Kikuchi patterns (Kainuma, 1955). The intensity profile across the line is calculated in the case of magnesium oxide. A matrix formulation of the many-beam dynamical theory is used in the calculation, where three beams of elastically scattered electrons and three beams of inelastically scattered electrons are taken into account. The result of the calculation is qualitatively in agreement with the observation.

Intensity formula of Kikuchi patterns

A number of photographs of diffraction patterns from magnesium oxide were taken by Uyeda & Nonoyama (1965*a*). In the diffraction patterns the unindexed line runs along the middle line of the 200 Kikuchi band as shown in Fig. 1. The intensity of this line becomes appreciable near the Bragg condition for the 400 reflexion.

The 000, 200 and 400 reflexions are strong in this case. Therefore, these three waves are taken into account in the theory. Their wave vectors are denoted by $\mathbf{k}_O, \mathbf{k}_H, \mathbf{k}_{2H}$ and the amplitudes by u_O, u_H, u_{2H}, where **O** represents 000 and **H**, 200. These waves are excited by the vacuum incident wave with the wave vector $\mathbf{K}_O$, as shown in Fig. 2(*a*). The amplitude of the incident wave is normalized to unity.

The inelastically scattered waves produce the Kikuchi pattern and continuous background. We consider an inelastically scattered wave which propagates to the observation point on or near the unindexed line. The wave vector of this wave is denoted by $\mathbf{K}'_O$ and its amplitude on the exit surface is normalized to unity. This wave is connected with the crystal waves taking account of three waves, $\bar{2}00$, 000 and 200. These waves have the wave vectors $\mathbf{k}'_{-H}, \mathbf{k}'_O, \mathbf{k}'_H$ and the amplitudes u'_{-H}, u'_O, u'_H as shown in Fig. 2(*b*).

The intensity of the Kikuchi pattern is given as a function of $\mathbf{K}_O$ and $\mathbf{K}'_O$. For wedge-shaped crystals it is written as follows (Kainuma & Kogiso, 1967),

$$J(\mathbf{K}'_0;\mathbf{K}_0) \propto \sum_{h,g} \sum_{h',g'} \frac{S(\mathbf{b}_{gg'}, \mathbf{b}_{hh'})}{b^2_{gg'} \cdot b^2_{hh'}} \cdot I_{hg} \cdot I'^{*}_{h'g'} \cdot \qquad (1)$$

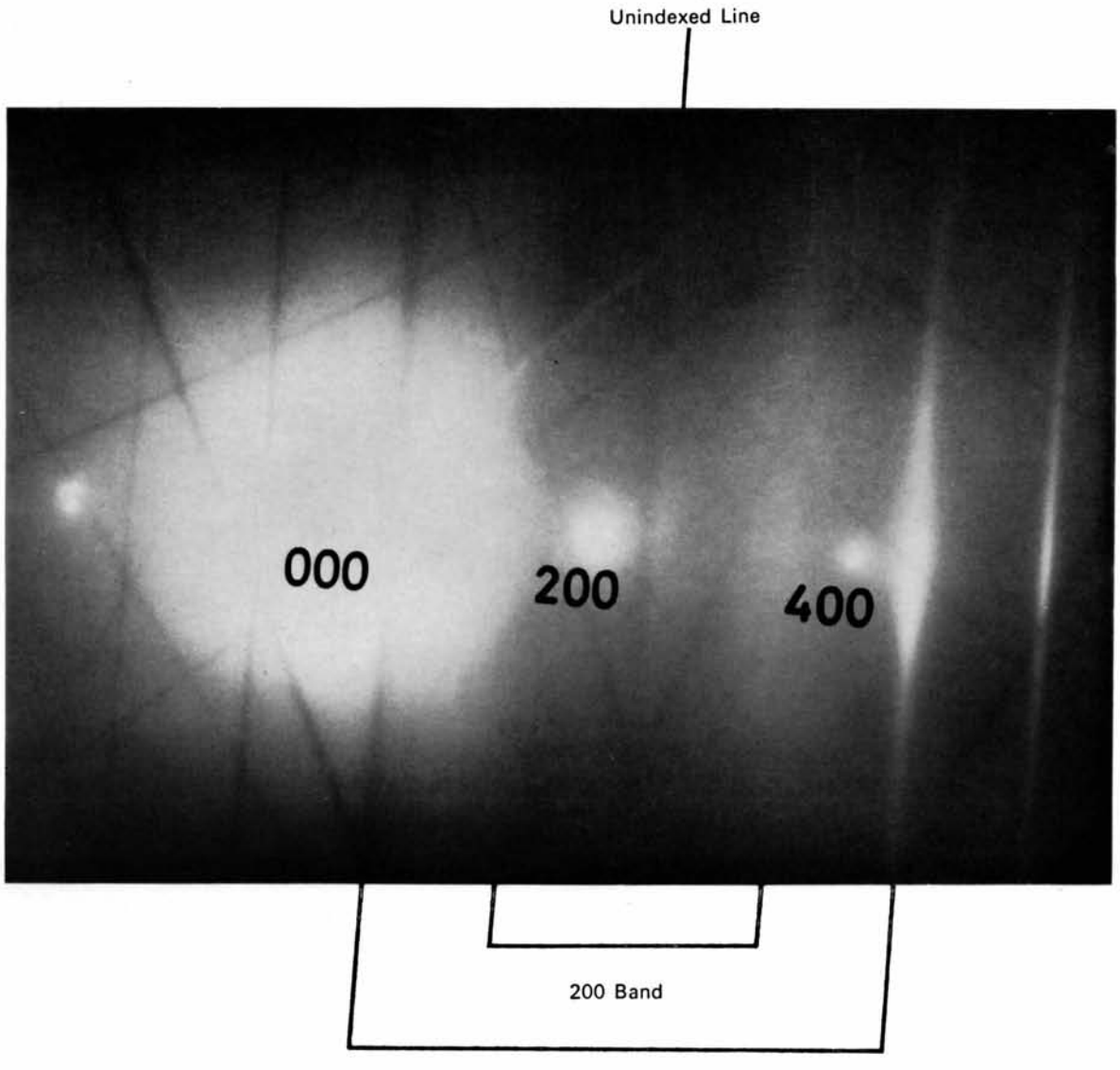

Fig. 1. Diffraction pattern from magnesium oxide for $\delta \simeq 0{\cdot}09$ Å^{-2} or $\Delta\theta/(\theta_B)_H \simeq 0{\cdot}42$. The unindexed line has an excess–deficient structure. (By courtesy of Professor Ryozi Uyeda.)

[*To face p.* 81

The factor S in the formula (1) is the structure factor of the Kikuchi pattern (Kainuma, 1955). The wave vector $\mathbf{b}_{gg'}$ is the scattering vector defined as

$$\mathbf{b}_{gg'}=\mathbf{k}_g-\mathbf{k}'_{g'}\,. \tag{2}$$

The factors I_{hg} and $I'_{h'g'}$ are defined as

$$\begin{aligned} I_{hg} &= \sum_{v} u_g^{(v)*}\,.\,u_h^{(v)}\,,\\ I'_{h'g'} &= \sum_{v'} u_{g'}^{\prime(v')*}\,.\,u_{h'}^{\prime(v')}\,, \end{aligned} \tag{3}$$

where v and v' specify the branches of the dispersion surface. It should be noted that the formula (1) is derived by taking into account only a single inelastic scattering. In the present problem, **h** and **g** stand for **O**, **H** and **2H**, and **h'** and **g'**, for $\bar{\mathbf{H}}$, **O** and **H**.

If the observation point lies near the 200 reflexion spot, the terms with small values of $b_{gg'}$ and $b_{hh'}$ are dominant in the summation. Thus the intensity formula (1) can be reduced to

$$J(\mathbf{K}'_0;\mathbf{K}_0)\propto \sum'_{h,g,h',g'} I_{hg}\,.\,I'^{*}_{h'g'}\,, \tag{4}$$

where the summation is taken over **g**, **g'**, **h** and **h'**, which satisfy the relation

$$\mathbf{g}'-\mathbf{g}=\mathbf{h}'-\mathbf{h}=\bar{2}00\,. \tag{5}$$

In the derivation of formula (4), the term $S(\mathbf{b}_{gg'}, \mathbf{b}_{hh'})/b^2_{gg'}\,.\,b^2_{hh'}$ is regarded as constant.

Elements I_{hg} and $I'_{h'g'}$

The matrix formulation of the many-beam dynamical theory of electron diffraction was developed by several authors (Niehrs & Wagner, 1955; Sturkey, 1957; Niehrs, 1959; Fujimoto, 1959; Kogiso & Kainuma, 1967). According to Kogiso and Kainuma, the elements I_{hg} and $I'_{h'g'}$ can be derived without solving the equation of the dispersion surface, as follows:

$$I_{hg}=D_{hg}/D\,, \tag{6}$$

where

$$D_{hg}=-\begin{vmatrix} 0 & (\boldsymbol{E})_{0g} & (\boldsymbol{M})_{0g} & (\boldsymbol{M}^2)_{0g}\\ (\boldsymbol{E})_{h0} & s_0 & s_1 & s_2\\ (\boldsymbol{M})_{h0} & s_1 & s_2 & s_3\\ (\boldsymbol{M}^2)_{h0} & s_2 & s_3 & s_4 \end{vmatrix} \tag{7}$$

and

$$D=\begin{vmatrix} s_0 & s_1 & s_2\\ s_1 & s_2 & s_3\\ s_2 & s_3 & s_4 \end{vmatrix}\,. \tag{8}$$

The matrices $\boldsymbol{E}$ and $\boldsymbol{M}$ in equation (7) are given as

$$\boldsymbol{E}=\begin{pmatrix} 1 & 0 & 0\\ 0 & 1 & 0\\ 0 & 0 & 1 \end{pmatrix} \tag{9}$$

and

$$\boldsymbol{M}=\begin{pmatrix} p_0 & v_{-H} & v_{-2H}\\ v_H & p_H & v_{-H}\\ v_{2H} & v_H & p_{2H} \end{pmatrix}\,. \tag{10}$$

In equation (10) v_g is the Fourier coefficient of the crystal potential expressed in Å^{-2}, and p_g is the parameter defined by

$$p_g=\kappa^2-\boldsymbol{\kappa}_g^2\,, \tag{11}$$

where

$$\boldsymbol{\kappa}_g=\boldsymbol{\kappa}_0+\mathbf{g}\,. \tag{12}$$

The wave vector $\boldsymbol{\kappa}_0$ has the same tangential component to the crystal surface as the wave vector $\mathbf{K}_O$, and has the magnitude $\kappa_0=\kappa=(K_O^2+v_O)^{\frac{1}{2}}$. The symbol s_n in equations (7) and (8) denotes the trace of the nth power of the matrix $\boldsymbol{M}$, *i.e.*

$$s_n=\mathrm{Spur}\,(\boldsymbol{M}^n)\,. \tag{13}$$

A formula with the same form as equation (6)

$$I'_{h'g'}=D'_{h'g'}/D' \tag{14}$$

is obtained for the expression of $I'_{h'g'}$, if $\boldsymbol{M}$ and s_n in equations (7) and (8) are replaced by $\boldsymbol{M}'$ and s'_n, respectively, where

$$\boldsymbol{M}'=\begin{pmatrix} p'_{-H} & v_{-H} & v_{-2H}\\ v_H & p'_0 & v_{-H}\\ v_{2H} & v_H & p'_H \end{pmatrix} \tag{15}$$

and

$$s'_n=\mathrm{Spur}\,(\boldsymbol{M}'^n)\,. \tag{16}$$

In equation (15) $p'_{g'}$ is defined as

$$p'_{g'}=\kappa'^2-\boldsymbol{\kappa}'^2_{g'}\,, \tag{17}$$

where

$$\boldsymbol{\kappa}'_{g'}=\boldsymbol{\kappa}'_0+\mathbf{g}'\,. \tag{18}$$

The wave vector $\boldsymbol{\kappa}'_0$ has the same tangential component to the crystal surface as the wave vector $\mathbf{K}'_O$, and has the magnitude $\kappa'_0=\kappa'=(K'^2_O+v_O)^{\frac{1}{2}}$.

The diagonal elements of the matrices $\boldsymbol{M}$ and $\boldsymbol{M}'$ satisfy the following relations:

$$\begin{aligned} p_0 &= 0\,,\\ p_H &= \tfrac{1}{2}\,.\,p_{2H}+H^2 \end{aligned} \tag{19}$$

and

$$\begin{aligned} p'_0 &= 0\,,\\ p'_{-H} &= \tfrac{1}{2}\,.\,(p'_{-H}-p'_H)-H^2\,. \end{aligned} \tag{20}$$

The following parameters δ and δ' are used as abbreviations:

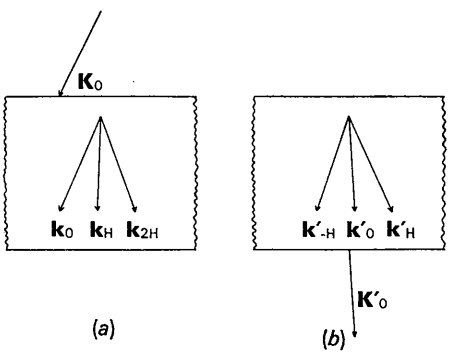

Fig. 2. Schematic diagram of waves. (*a*) Incident wave in vacuum and elastically scattered waves in the crystal. (*b*) Inelastically scattered wave towards the observation point and crystal waves connected with it.

$$\delta = \tfrac{1}{2} \cdot p_{2H} = -2\mathbf{K}_H \cdot \mathbf{H},$$
$$\delta' = \tfrac{1}{2} \cdot (p'_{-H} - p'_H) = 2\mathbf{K}'_O \cdot \mathbf{H}, \qquad (21)$$

where $\mathbf{K}_H$ is the wave vector of the Hth wave in vacuum. The second expressions in equations (21) follow since $\mathbf{H}$ is parallel to the crystal surfaces.

The parameter δ is determined by the direction of the incident wave and δ' by the observation point. These parameters are approximately proportional to the angular deviations $\Delta\theta$ and $\Delta\theta'$ as follows,

$$\delta = \frac{1}{d_H^2} \cdot \frac{\Delta\theta}{(\theta_B)_H},$$
$$\delta' = \frac{1}{d_H^2} \cdot \frac{\Delta\theta'}{(\theta_B)_H}, \qquad (22)$$

where d_H and $(\theta_B)_H$ are respectively the interplanar spacing and the Bragg angle for $\mathbf{H}=200$. $\Delta\theta$ is the angular deviation of the incident beam from the exact Bragg position of the 400 reflexion, namely, $\Delta\theta=\theta-(\theta_B)_{2H}$, where θ is the glancing angle of the incident beam to the net plane $\mathbf{H}$ and $(\theta_B)_{2H}$ is the Bragg angle for $\mathbf{2H}=400$. $\Delta\theta'$ is the angle between $\mathbf{K}'_O$ and the net plane $\mathbf{H}$. $\Delta\theta'$ corresponds to the angular deviation of the observation point from the middle of the 200 band. If the observation point lies exactly in the middle of the band, we have $\Delta\theta'=0$. $\Delta\theta'$ is positive or negative according as the observation point lies on the side nearer to the 400 reflexion spot or to the incident spot.

The terms D_{hg} and D in equations (7) and (8) are written as polynomials of less than the 7th degree in the parameter δ. $D'_{h'g'}$ and D' are also written in δ'. The coefficients of these polynomials are defined by v_H, v_{2H} and H^2. Adopting the values $v_H=5{\cdot}42\times10^{-2}$ Å^{-2}, $v_{2H}=2{\cdot}52\times10^{-2}$ Å^{-2} and the lattice parameter $a=4{\cdot}2117$ Å, I_{hg} and $I'_{h'g'}$ are calculated as functions of δ and δ', respectively. The results are shown in Fig. 3. It should be noted that I_{hh} and $I'_{h'h'}$ are the intensities averaged over the thickness of h and h' reflexions, respectively, and that $\sum_h I_{hh}=1$ and $\sum_{h'} I'_{h'h'}=1$.

Intensity profiles

The intensity profiles across the unindexed line calculated by formula (4) are shown in Fig. 4 as functions

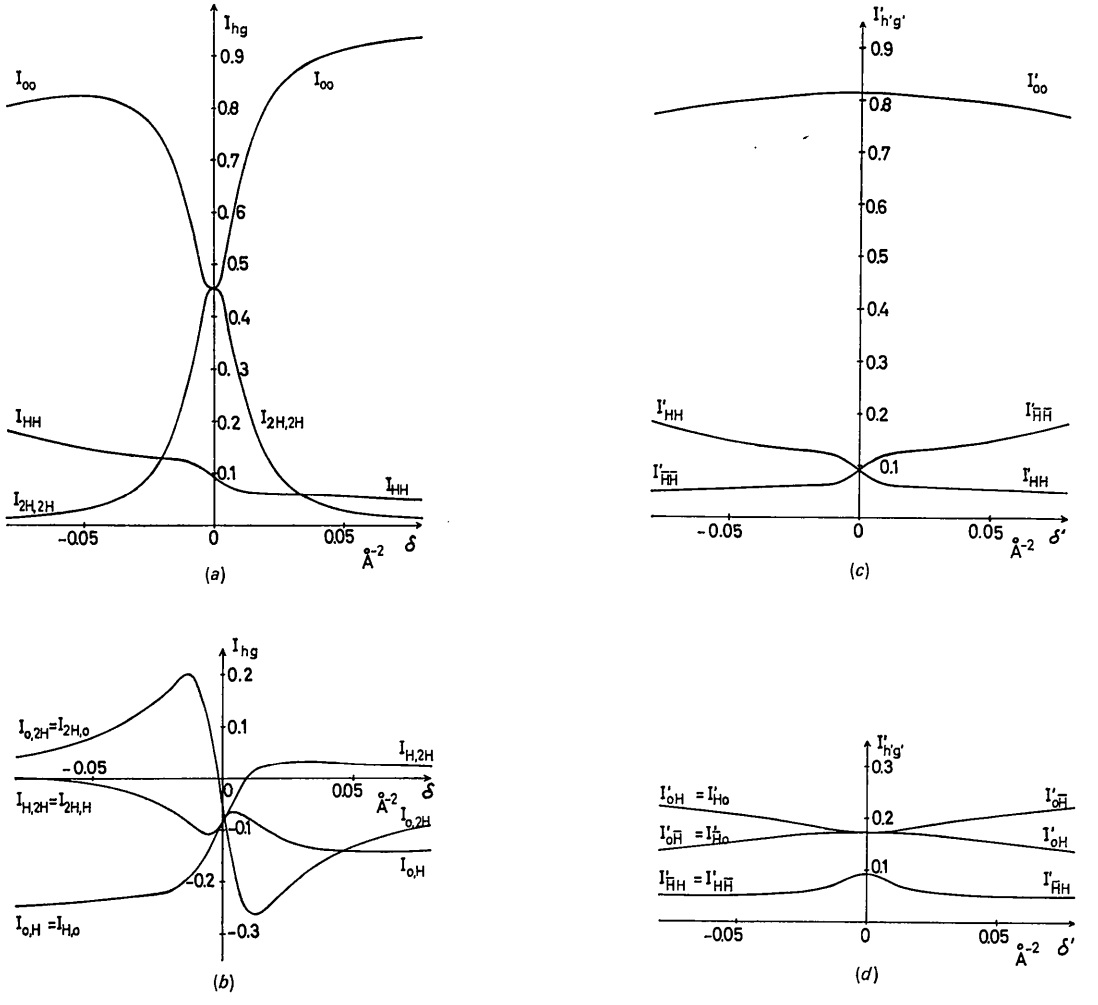

Fig. 3. Elements I_{hg} and $I'_{h'g'}$ as functions of δ and δ'.

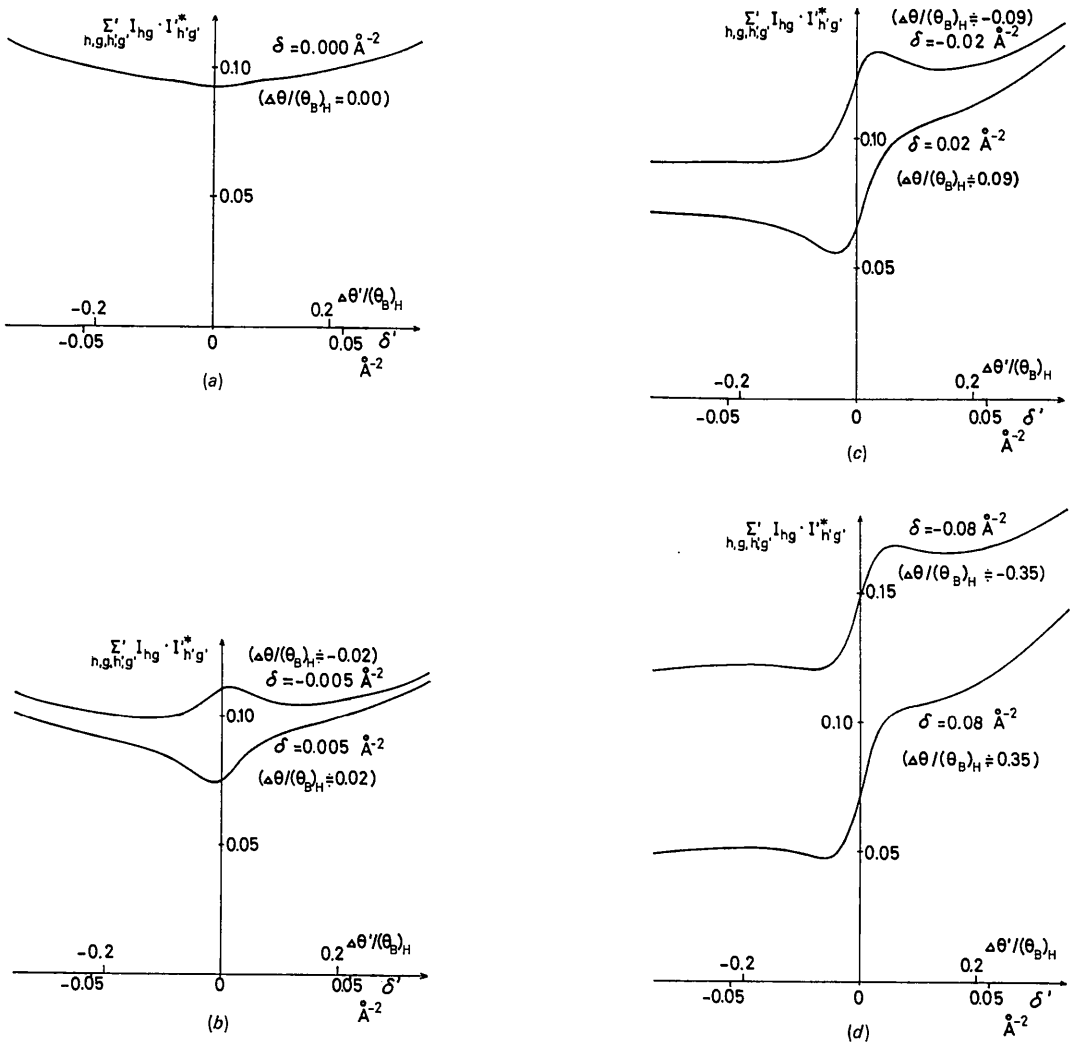

Fig. 4. Intensity profiles across the unindexed line for various values of δ.

of δ', or $\Delta\theta'/(\theta_B)_H$, for various values of δ, or $\Delta\theta/(\theta_B)_H$. Fig. 4(*a*) shows that the unindexed line is very faint when the Bragg condition for the 400 reflexion is exactly satisfied. For small values of $|\delta|$, the line appears as an excess or deficient line. It is excess or deficient respectively for negative or positive values of δ, as shown in Fig. 4(*b*).

For large values of $|\delta|$, the unindexed line has an excess-deficient structure as shown in Fig. 4(*c*) and (*d*). This structure is observed in Fig. 1. The deficient side of the line in Fig. 1 is found nearer to the incident spot, and the breadth of the line is about $(1/10)(\theta_B)_H$, which is the same order as the Bragg width of the 400 reflexion. These features are in agreement with those in Fig. 4(*c*) and (*d*).

The authors wish to express their sincere thanks to Professor Ryozi Uyeda for his helpful discussions. This work was partially supported by the Grants-in-Aid for Cooperative Scientific Research from the Ministry of Education.

References

FUJIMOTO, F. (1959). *J. Phys. Soc. Japan*, **14**, 1558.
ICHINOKAWA, T. & FUKANO, Y. (1952). Reported at annual meeting Phys. Soc. Japan.
KAINUMA, Y. (1955). *Acta Cryst.* **8**, 247.
KAINUMA, Y. & KOGISO, M. (1967). In preparation.
KOGISO, M. & KAINUMA, Y. (1967). In preparation.
NIEHRS, H. & WAGNER, E. H. (1955). *Z. Phys.* **143**, 285.
NIEHRS, H. (1959). *Z. Naturforsch.* **14**a, 504.
PFISTER, H. (1953). *Ann. Phys. Lpz.* **11**, 239.
STURKEY, L. (1957). *Acta Cryst.* **10**, 858.
UYEDA, R. & NONOYAMA, M. (1965*a*). *Japan. J. Appl. Phys.* **4**, 498.
UYEDA, R. & NONOYAMA, M. (1965*b*). Private communication.